

The Stratigraphy of Compound Sand Blows at Sites of Recurrent Liquefaction: Implications for Paleoseismicity Studies

Brett W. Maurer, a) M.EERI, Russell A. Green, b) M.EERI, Liam M. Wotherspoon, c) M.EERI, and Sarah Bastind)

Paleoliquefaction studies provide valuable information for seismic hazard analyses in areas where the return period of moderate to large events is longer than the duration of the historical earthquake catalog (e.g., Central-Eastern and Pacific Northwest United States). Toward this end, paleoliquefaction studies require accurate and detailed assessments of individual features and of the extent of the paleoliquefaction field for the event, with the difficulty of accurately interpreting field observations increasing in areas where recurrent liquefaction was triggered by spatiotemporally clustered paleo events. Accordingly, undisturbed features formed by recurrent liquefaction during the 2010–2011 Canterbury, New Zealand, earthquake sequence were studied to facilitate interpretation of paleoliquefaction analogs. Silt drapes demarcated multiple episodes of liquefaction in the sand blows, with the thickness of the silt drapes correlating to the fines content of the liquefied source stratum. However, no ubiquitous trends in the spatial sorting of grain sizes in the coarser fraction of the ejecta underlying silt drapes were observed. This study provides a modern analog to recurrent paleoliquefaction evidence and has important implications for interpretation of seismic hazards. [DOI: 10.1193/041818EQS097M]

INTRODUCTION

The objective of the study presented herein is to provide insights into performing paleoliquefaction studies in regions impacted by multiple earthquakes that triggered recurrent liquefaction over short time intervals. Paleoliquefaction studies utilize liquefaction features preserved in the geologic record and can provide information about the locations, magnitudes, and recurrence rates of prehistoric or preinstrumental earthquakes (e.g., Obermeier 1989, 1996, Tuttle 2001, Tuttle et al. 2002a, 2002b, Obermeier et al. 2005, Olson et al. 2005a, 2005b, Green et al. 2005, Cox et al. 2007, Counts and Obermeier 2012, Tuttle and Hartleb 2012, Maurer et al. 2015c, Bastin et al. 2015, 2016). Such studies are often employed in areas where the return period of moderate to large events is longer than the duration of the catalog of historical seismicity [e.g., Central-Eastern United States

a) Department of Civil and Environmental Engineering, University of Washington, Seattle, WA

b) Department of Civil and Environmental Engineering, Virginia Tech, Blacksburg, VA; Email: rugreen@vt.edu

c) Department of Civil and Environmental Engineering, University of Auckland, Auckland, New Zealand

d) Department of Civil and Natural Resources Engineering, University of Canterbury, Christchurch, New Zealand



Figure 1. Map of CEUS showing locations of regional paleoliquefaction data sets in the CEUS Seismic Source Characterization (SSC) Project. These data sets were inputs to probabilistic seismic hazard analyses for nuclear facilities in the region (adapted from Tuttle and Hartleb 2012).

(CEUS) and Pacific Northwest United States]. For example, paleoliquefaction features have been identified in ten regions of the CEUS, as shown in Figure 1, with the estimated locations and magnitudes of the causative paleoearthquakes used to define seismic source zones for probabilistic seismic hazard analyses for nuclear facilities [Nuclear Regulatory Commission (NRC) 2012].

The accurate interpretation of paleoliquefaction features relies on (1) their identification within the geologic record, (2) determination of their age, and (3) constraint of the ground motions under which they formed (Obermeier et al. 1991, Sims and Garvin 1995, Obermeier 1996, Tuttle 2001, Tuttle et al. 2002a, 2002b). Central to estimating the magnitude of a paleoearthquake is establishing the areal extent of liquefaction in the impacted region (i.e., the size of the "liquefaction field"), as determined from the identification of paleoliquefaction features resulting from a common causative event. Developing such an understanding can be hampered by uncertainties about whether observed features formed during a single large earthquake or multiple spatiotemporally clustered events that were part of a sequence. For example, it is known that three mainshocks between December 1811 and February 1812 collectively triggered widespread liquefaction in the New Madrid Seismic Zone (NMSZ) in the Central United States (e.g., Obermeier 1989). From the spatial

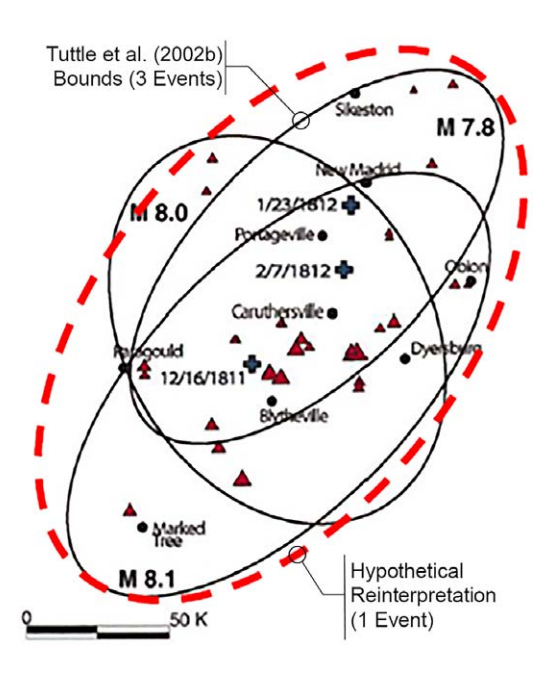


Figure 2. Reinterpretation of bounds of the liquefaction fields from the 1811–1812 New Madrid events as being induced by a single earthquake (adapted from Tuttle et al. 2002b and Hough 2011).

distribution and stratigraphy of sand blows, Tuttle et al. (2002b) interpreted the liquefaction fields associated with each mainshock, as shown in Figure 2. However, if the liquefaction fields were reinterpreted as being caused by a single earthquake, or as being augmented by additional spatially distributed large aftershocks, the back-calculated magnitude(s) of the event(s) could be decidedly different (e.g., Hough 2011). As a result, design ground motions derived from seismic hazard analyses that use data from paleoliquefaction studies as input can potentially range significantly depending on the field interpretations of the paleoliquefaction features, impacting engineering practice and public safety.

A large body of literature exists pertaining to paleoliquefaction field interpretation, including comprehensive overviews (e.g., Obermeier et al. 2001, 2005) and numerous case studies outlining causative paleoearthquake magnitudes and epicentral locations (e.g., among others, Obermeier and Dickenson 2000, Tuttle 2001, Talwani and Schaeffer 2001, Tuttle et al. 2002a, 2002b, 2005, Cox et al. 2007, and Bastin et al., 2016). Research focusing on the interpretation of recurrent liquefaction, however, is very limited. Because the accuracy of the interpretation of the causative paleoearthquake depends greatly on differentiation of liquefaction episodes, a reliable method for their identification could help to resolve paleoseismic enigmas, thereby reducing the uncertainty of inputs needed for seismic hazard analyses. Several researchers have suggested from visual inspection of paleoliquefaction features in the NMSZ (Saucier 1989, Tuttle et al. 2002b) and modern features in California (Sims and Garvin 1995) that soil grains tend to sort by size within deposits of liquefaction

ejecta, fining both upwards and laterally from the source vent, and that such trends are an identifying feature of episodic liquefaction. To further the efforts to determine whether recurrent liquefaction episodes can be discerned from the structure and grain-size distribution of vented sediments, this study trenched compound sand blows at four sites of recurrent liquefaction triggered by the 2010–2011 Canterbury, New Zealand, earthquake sequence (CES). The structures of compound features exposed during trenching were mapped in detail, and extensive sampling of the ejecta was undertaken to analyze spatial trends in particle-size gradation. This study is the first to quantitatively analyze such trends in extensive detail and addresses a critical need in paleoliquefaction interpretation of compound sand blows.

In the following, the geologic and seismologic setting of the CES is briefly summarized. This is followed by a description of the field investigation and sampling methodology. The morphology and grain-size distribution patterns of sand-blow structures are then analyzed in detail, with discussion of the implications for paleoseismicity studies.

GEOLOGIC AND SEISMOLOGIC SETTING OF THE CES

The four sites investigated in this study are within or near the city of Christchurch, located on the east coast of New Zealand's South Island. The central and eastern suburbs of the city are predominantly underlain by loosely consolidated alluvial sands and silts that are locally interbedded with dune, estuarine, and foreshore sands to silts (Brown et al. 1995). The alluvial sediments were initially deposited by the Waimakariri River, which regularly flooded and avulsed across the region prior to European settlement. The deposits have subsequently been reworked and redeposited by the meandering Avon, Heathcote, and Styx Rivers that also flooded and avulsed across the area (Brown et al. 1995). The dune, estuarine, and foreshore sands to silts were deposited during sea level regression following a mid-Holocene highstand that reached up to 3 km inland of the central city at 6,500 years before present (Brown et al. 1995). River realignments and land reclamation projects following the European settlement of Christchurch in the mid-1800s resulted in the infilling of many low-lying areas with loose, low-plasticity sediments (e.g., Wotherspoon et al. 2012).

While the liquefaction susceptibility of the loose deposits and fill to the east of the city center had been recognized prior to the CES (Environment Canterbury 2004), the only previously documented case of liquefaction was in the township of Kaiapoi, north of Christchurch, during the 1901 Cheviot earthquake (e.g., Berrill et al. 1994). Paleoliquefaction features have since been discovered in the wider Christchurch area (Tuttle 2012, Maurer et al. 2015c, Bastin et al. 2016) and provide evidence of earthquake(s) prior to European settlement, but the source and size of the causative events are uncertain.

The 2010–2011 CES initiated with the 4 September 2010 M_w 7.1 Darfield earthquake and included twelve other $M_w \geq 5.0$ events epicentrally located within 20 km of Christchurch (GeoNet 2012). While at least ten of these events are known to have triggered liquefaction in Christchurch (Quigley et al. 2013), the 22 February 2011 M_w 6.2 Christchurch earthquake was by far the most damaging because of its rupture plane being located directly beneath the southern environs of Christchurch (e.g., Beavan et al. 2011). An extensive body of literature exists pertaining to the CES, including numerous aspects of liquefaction incidence and prediction (e.g., Cubrinovski and Green 2010, Cubrinovski et al. 2011a, 2011b, 2012, Green et al. 2011a, 2011b, Kam et al. 2011, Wotherspoon et al. 2012, Robinson et al. 2014,

van Ballegooy et al. 2014, Maurer et al. 2014, 2015a, 2015b); the reader is referred to these works and others for a complete overview of the CES. Of relevance to paleoliquefaction research, the geomorphology of soil deposits, severity of liquefaction, and relative timing of the CES events make them directly analogous to paleoearthquake clusters previously documented in the NMSZ and elsewhere. As such, the CES provides a unique modern analog to recurrent paleoliquefaction evidence.

METHODOLOGY

Beginning in August 2011, a series of trenches were excavated at sites of known recurrent liquefaction across eastern Christchurch and its environs (Figure 3). Episodic liquefaction was documented at these sites during the earthquake sequence from ground reconnaissance and high-resolution satellite imagery (New Zealand Geotechnical Database 2012). As mapped in Figure 3, trenches were excavated at sites located in Ferrymead (FMD) near the Heathcote River, in South Kaiapoi (KAI) near the Kaiapoi River, and in Dallington (DAL) and Burwood (BUR), both in close proximity to the Avon River. All of these sites are located on flat ground and are known to not have been impacted by lateral spreading.

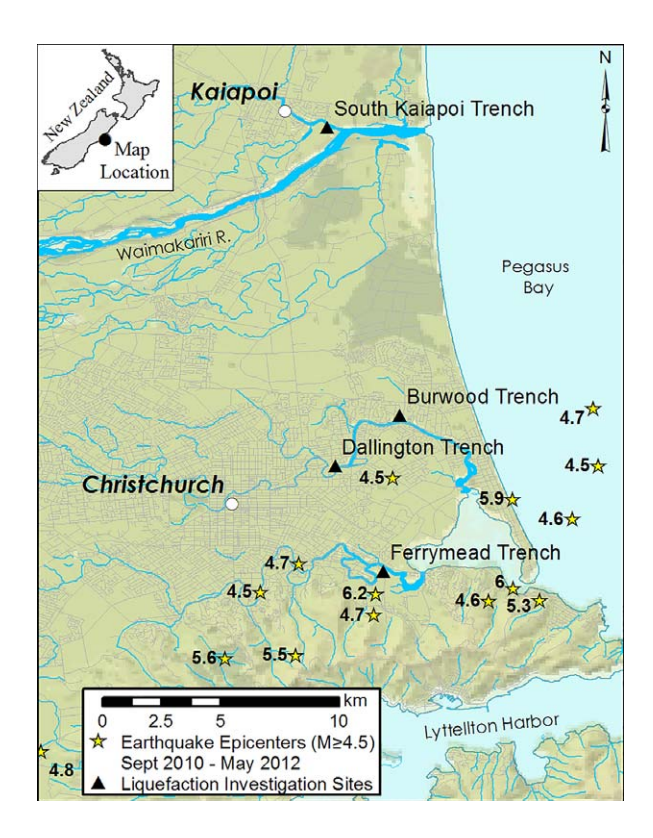


Figure 3. Liquefaction investigation sites and local earthquake epicenters, $M_w \ge 4.5$ (September 2010–May 2012). Note: M_w 7.1 Darfield earthquake is epicentrally located ~40 km west of central Christchurch.

As such, the investigated features are assumed not to have been influenced by surface topography. The epicenters of CES events having $M_w \ge 4.5$ are also shown in Figure 3, with $M_w \sim 4.5$ being the smallest magnitude known to have triggered liquefaction worldwide (e.g., Green and Bommer 2019). Several notable events, including the epicenter and surface fault rupture of the $M_w 7.1$ Darfield earthquake, plot beyond the extents of Figure 3. Satellite images of each investigation site (captured 24 February 2011) are presented in Figure 4; the presence of widespread and/or severe liquefaction ejecta is readily apparent at each site.

The investigated liquefaction features were free of anthropogenic disturbance because of their locations in pastures (FMD, KAI) and vacant residential properties that were abandoned early in the earthquake sequence (DAL, BUR), but they were open to the elements. With the exception of the BUR trench, trenches cross-cut liquefaction features formed from multiple episodes of liquefaction venting onto the ground surface through a common dike. BUR is located at a site known to have liquefied multiple times but is unique in that the liquefaction dike terminated beneath the ground surface, producing a buried lateral sill of liquefied



Figure 4. Satellite imagery (captured 24 February 2011) of liquefaction investigation sites located in (a) South Kaiapoi (-43.388458, 172.671662), (b) Burwood (-43.498080, 172.700030), (c) Dallington (-43.517318, 172.675461), and (d) Ferrymead (-43.557242, 172.693751). Imagery adapted from Canterbury Geotechnical Database (2012).

material and resulting in a "sand blister" on the ground surface (e.g., Bucci et al. 2017). Such features could be especially important in paleoseismic analyses because they are protected from erosion and may thus better preserve the seismic record. The structures of all four liquefaction features were mapped in detail, and extensive sampling of the ejecta was undertaken to analyze trends in particle-size gradation via sieve analysis and laser diffraction (Malvern Mastersizer 3000; Malvern Panalytical, Malvern, United Kingdom).

RESULTS AND DISCUSSION

STRUCTURE OF SANDBLOW DEPOSITS

The KAI trench intersected a liquefaction feature with five sequences of coarse ejecta overlain by silt laminations (or "drapes") approximately 1 cm thick (mapped in Figure 5). We interpret each coarse layer-silt drape pair as representing a separate episode of liquefaction. The feature is mapped in Figure 5, wherein we label the (1) interpreted five episodes, or

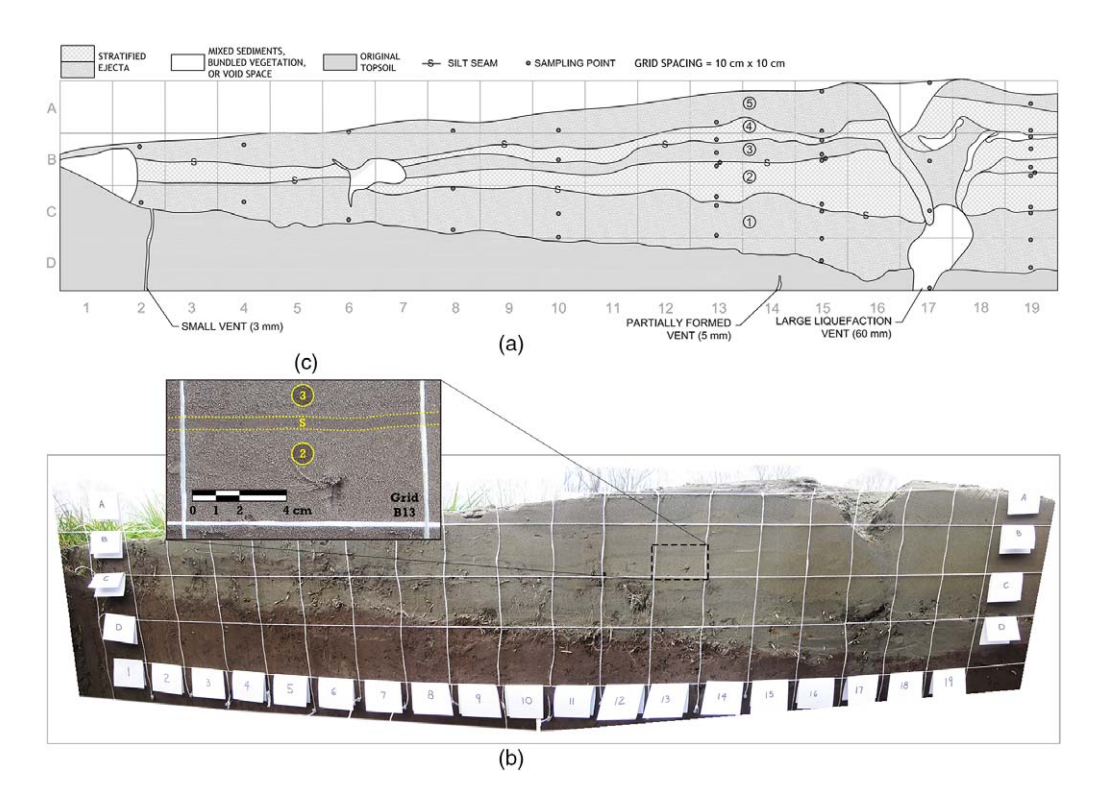


Figure 5. (a) Log of the eastern wall at the KAI trench showing at least five sand-venting episodes of liquefaction separated by silt drapes (labeled "S"); sampling points identified in the log are analyzed and discussed in the text. (b) Photograph of the eastern wall at the KAI trench prior to sampling (overlaid with a $10 \times 10 \,\mathrm{cm}$ grid); interevent silt drapes are visible in the photo (e.g., most clearly in grid cells B11 through B14). (c) Photograph of grid cell B13 in detail, showing one silt drape and two episodes of liquefaction.

units, of liquefaction ejecta; (2) silt drapes, which cap units of ejecta, distinguishing them from overlying successive units; and (3) locations of 46 grain-size distribution samples to be analyzed and discussed subsequently. Also presented in Figure 5 are photographs of the KAI trench, including a detailed view of the morphology and sequencing of a representative silt drape.

The silt drapes, which cap individual layers of coarser ejecta up to 10 cm thick, suggest an interval of placid water deposition following a period of turbulent rupture. Silt drapes were found to commonly contain 10-µm-sized particles up to 5% by volume and to have particle sizes less than 2 µm. Applying the fundamentals of Stoke's Law, and assuming spherical particles, the smallest of these grains is estimated to have a terminal settling velocity less than 1 cm/hr. This suggests that significant time was required for the silt drapes to form and that multiple silt drapes within a blow structure are unlikely to have been produced by multiple "pulses" of shaking during a single earthquake. As such, silt drapes were found to be an identifying feature of episodic liquefaction, a finding consistent with previous observations of sand blows in the field (Sims and Garvin 1995, Tuttle et al. 2002b, Quigley et al. 2013, Tuttle et al. 2017).

The liquefaction features intersected by the DAL and FMD trenches exhibited evidence for three and four episodes of liquefaction, respectively (mapped in Figures 6 and 7). As

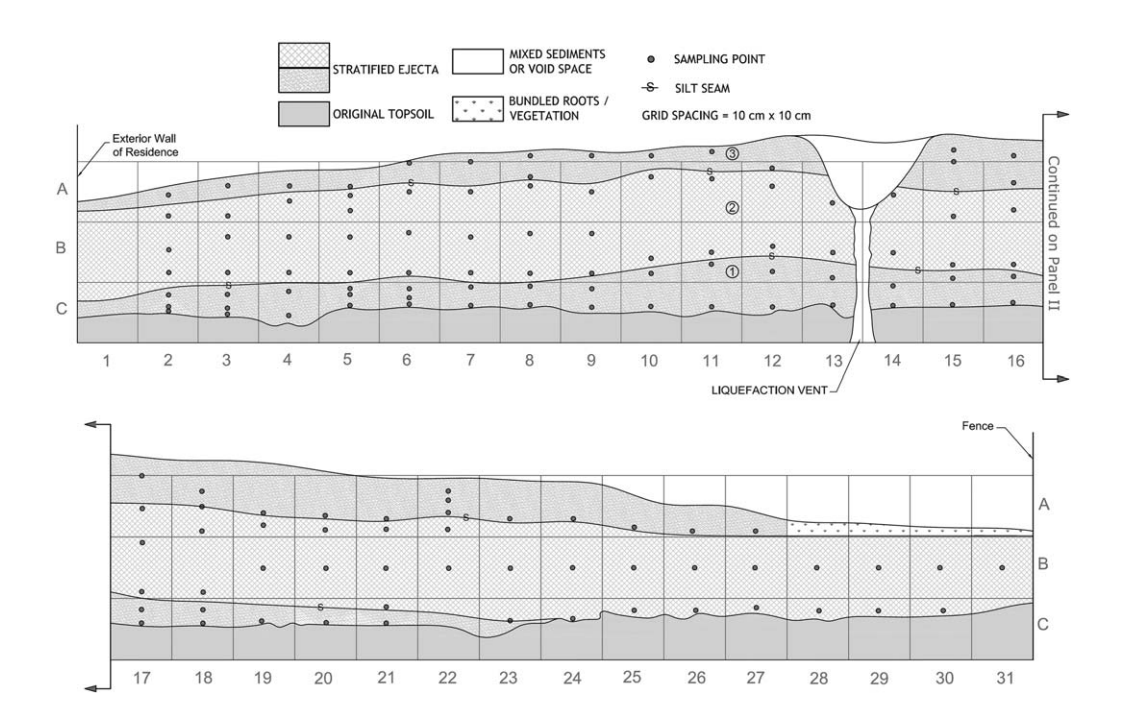


Figure 6. Log of the eastern wall at the DAL trench showing at least three sand-venting episodes of liquefaction separated by silt drapes (labeled "S"); sampling points identified in the log are analyzed and discussed in the text.

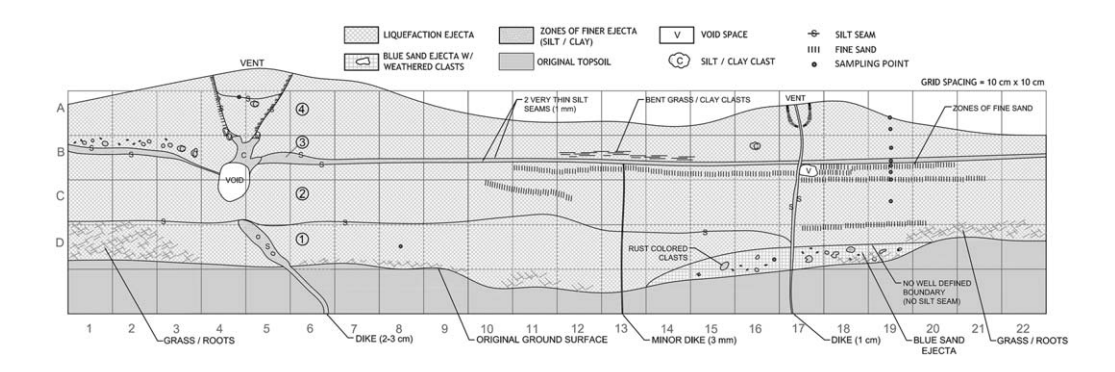


Figure 7. Log of the western wall at the FMD trench showing at least four sand-venting episodes of liquefaction separated by silt drapes (labeled "S"); sampling points identified in the log are analyzed and discussed in the text.

with the KAI trench, the interpreted units of ejecta, the interevent silt drapes, and the locations of grain-size distribution samples analyzed (and discussed subsequently) are labeled in Figures 6 and 7. A total of 153 such samples were collected from the DAL and FMD features.

The BUR trench, which intersected the center of the liquefaction blister, revealed two distinct silt drapes in the sill structure, as mapped in Figure 8. Gradations of samples collected from the silt drapes and from the coarse ejecta regions in the BUR feature are shown in Figure 9. It can be seen that depositional sorting of the finer silt drapes from the coarser grains occurred despite a lack of venting onto the ground surface, indicating that evidence of recurrent paleoliquefaction can be gathered from these unique and important structures.

Silt seam particle-size gradations were compared with those of the underlying layer of coarser ejecta for all the investigation trenches. Pairs of samples from the silt seam and underlying coarser ejecta were obtained at the same lateral distance from the vent, as depicted in

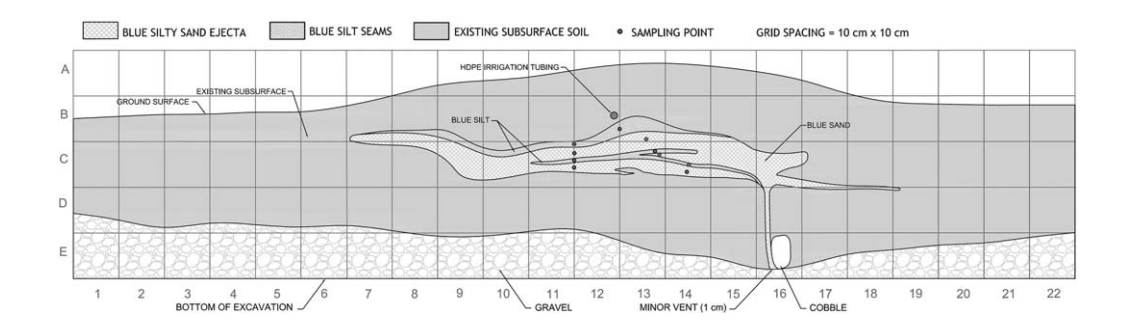


Figure 8. Log of the southwestern wall at the BUR trench. Depositional sorting and multiple episodes of liquefaction are evident despite a lack of venting onto the ground surface. Sampling points identified in the log are analyzed and discussed in the text.

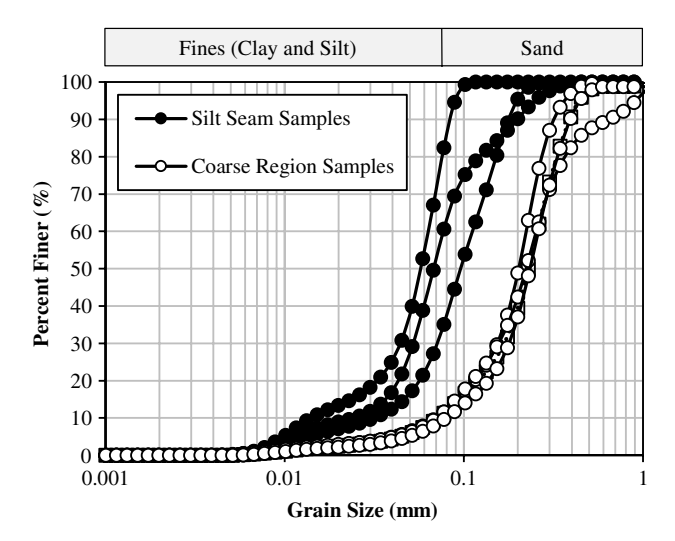


Figure 9. Comparison of silt-seam and coarse ejecta grain-size distributions in the BUR trench.

Figures 5–8. Sample pairs were compared by computing the ratio of effective particle-size diameters D_5 , D_{10} , D_{60} , and D_{90} in the silt seam to those in the underlying layer. Accordingly, ratios less than 1.0 indicate a finer particle-size gradation in the silt seam. The average D_5 , D_{10} , D_{60} , and D_{90} ratios were 0.52, 0.61, 0.68, and 0.80, respectively, for the sample pairs. Thus, silt drapes are discernable because of their finer grain-size distributions (and visually so, as shown in Figure 5c), particularly in the finest effective particle-size diameters, rather than being distinct because of differences in coloration from weathering or any other phenomena.

Silt drapes in the liquefaction features exposed in the DAL and FMD trenches were significantly thinner (~ 2 mm) than those in the KAI and BUR structures (~ 8 mm) despite the coarser ejecta layers underlying the silt drapes being of comparable or greater thickness in the DAL and FMD features. The trenched sites are all located in areas containing recent fluvial sediments deposited by the Waimakariri River and reworked by local meandering rivers, and they thus exhibit uniform compositions and soil types. To evaluate whether variations in silt-drape thicknesses correlate with characteristics of the source material, vertical boreholes were augered in the floor of the DAL and KAI trenches to locate and sample the liquefied source strata. Borings in the other trenches were not possible because of the presence of a high ground-water table (FMD) and shallow hardpan (BUR). The suspected source strata in the DAL and KAI features were identified considering (1) cone penetration test data, which was used to quantify the likelihood of liquefaction triggering using several liquefaction-triggering models (e.g., Idriss and Boulanger 2008, Green et al. 2018); and (2) qualitative comparisons between borehole samples and the blow material at each site. The grain size distributions of liquefied source strata of the KAI and DAL trench features are shown in Figure 10. The KAI source stratum was found to contain ~45% silt-size particles ($<75 \mu m$), while the source stratum of the DAL feature contained only $\sim 14\%$ silt-sized particles. Variations in the thicknesses of the silt drapes therefore appear to be

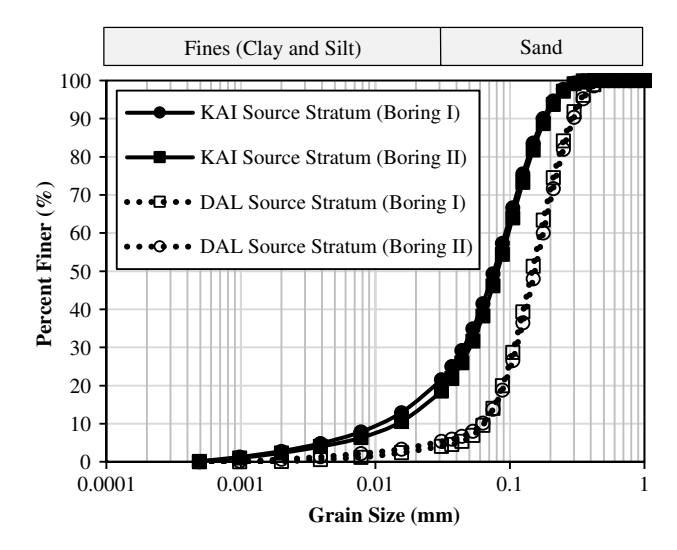


Figure 10. Grain-size distributions of liquefied source strata beneath the KAI and DAL trenches.

proportional to the fines content of the liquefied source stratum at these two sites, suggesting that the grain-size distributions of the liquefied source influence the sediment structure of the ejected material. Consequently, it is anticipated that silt drapes would not form at sites where the fines content of the liquefied stratum approaches small values. More specifically, it is hypothesized that there is a limiting fines content, below which particle sorting fails to produce a perceptible silt drape, or that if formed, the drape would be so thin that it would be susceptible to erosion and unlikely to be preserved in the geologic record. We note, however, that the source strata for all the sites studied had similar modes of deposition and geologic origin. As a result, it cannot be stated with certainty that compound sand boils formed from deposits having differing compositions and geomorphologic origins will have the same stratigraphies as the features studied herein. However, many deposits hosting paleoliquefaction features worldwide have similar compositions and geomorphologies as those presented in this study (i.e., non-to-low plastic fluvial deposits), and thus the features could be expected to have similar stratigraphies.

ANALYSIS OF GRAIN SIZE DISTRIBUTION PATTERNS

Given that the range of soils considered to be liquefiable is large (e.g., Ishihara 1985) and encompasses soils containing less fines than some of the soils that liquefied in Christchurch (Figure 11), silt drapes may not always be relied on to define recurrent paleoliquefaction. In the NMSZ, Tuttle et al. (2002b) trenched numerous paleoliquefaction features and observed that silt drapes were present only in some cases. When silt drapes were absent, the presence of repeating fining-upward units was interpreted as evidence of episodic liquefaction. These findings suggest that spatial trends in particle-size gradation, absent of silt drapes, may be critical for identifying recurrent liquefaction in some cases. To assess whether such

- A: "Potentially liquefiable" soil (Ishihara 1985)
- B: "Most liquefiable" soil (Ishihara 1985)
- C: Liquefied soil in Christchurch (this study)

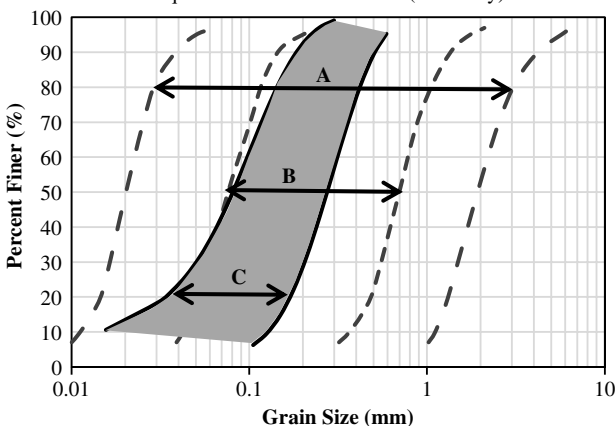


Figure 11. Grain-size distributions of liquefied soils in Christchurch, with boundaries for "most liquefiable" and "potentially liquefiable" soils (Ishihara 1985). Many liquefiable soils have fewer fines than those in Christchurch, and, consequently, some sand-boil structures would likely lack perceptible interevent drapes.

evidence is present in the Christchurch features, particle-size trends in the coarser fraction of the ejecta underlying the silt drapes are investigated.

Vertical and lateral trends in grain-size distributions in each trench were analyzed using more than 100 sample pairs recovered from the base and top (immediately below silt drape) of individual coarse-grained blow units at varying distances from the vent. Fining-upward trends were examined for the sample pairs by analyzing the ratios of effective particle diameters D₅, D₁₀, D₆₀, and D₉₀ in the upper-reaches of a blow unit to those at the base of the same unit. As such, ratios less than 1.0 indicate fining upward within a depositional unit. Vertical trends are shown in Figure 12 for the KAI (Figure 12a) and DAL (Figure 12b and 12c) trenches. Owing to the large number of samples in the DAL feature, vertical trends are parsed into those of the first (oldest) and second ejecta layers. As may be observed from Figure 12, there are no consistent trends in particle gradation in either the KAI or DAL features. While some sample pairs indicate that ejecta is fining upward, many show no spatial change in gradation, while others indicate that ejecta is finer at the base of a unit. Considering all sampling pairs in the KAI and DAL features, the average D₅, D₁₀, D₆₀, and D₉₀ ratios were 0.96, 0.91, 0.94, and 0.96, respectively. If blow units were fining upward as expected, this ratio would be significantly less than one.

Statistical *t*-tests (e.g., DeGroot and Schervish 2012) were used to assess whether the observed ratios are statistically significant. These tests compute the *P*-value, or probability, of obtaining an observed sample average if the null hypothesis is true (i.e., that no grain-size trends exist, in which case average ratios of one are expected). For the aforementioned D_5 , D_{10} , D_{60} , and D_{90} average ratios, the *P*-values are 0.42, 0.09, 0.12, and 0.23, respectively.

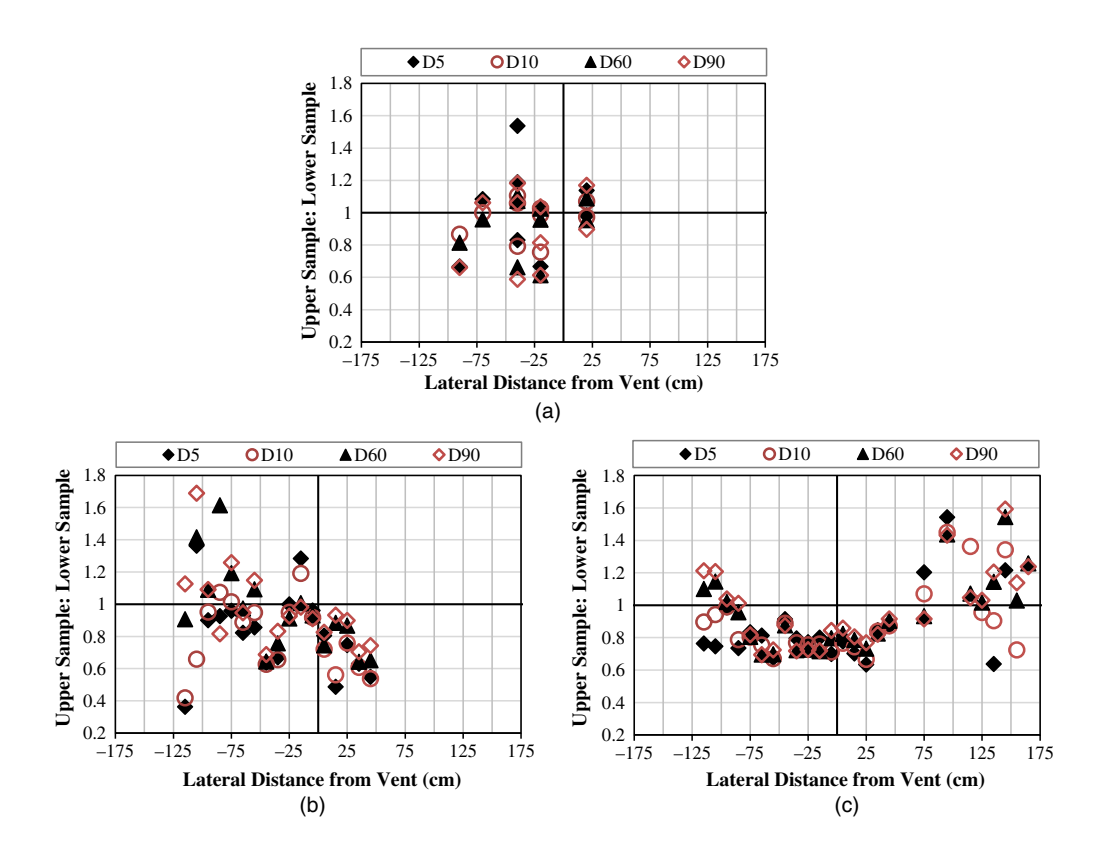


Figure 12. Analysis of particle-size trends in the vertical direction for the (a) KAI trench (all sample pairs), (b) DAL unit 1 (oldest ejecta layer), and (c) DAL unit 2 (second oldest ejecta layer). Data points represent the ratio of sample characteristics from the top of a depositional unit to those at the bottom. As such, values less than 1.0 indicate fining upward within a unit.

If the commonly used significance level of 0.05 is adopted, none of the observed ratios are significantly less than one (i.e., all *P*-values exceed 0.05). While some observed averages could become statistically significant if this criterion was relaxed, the results in general would still be inconclusive. In addition, no clear trend was identified in the fining-upward trends with lateral distance from the vent.

To identify fining-outward trends, the same effective particle diameters (i.e., D_5 , D_{10} , D_{60} , and D_{90}) were plotted versus lateral distance for each blow unit along lines of constant relative elevation within the unit (top or bottom of ejecta layer). Lateral trends are shown for the KAI and DAL features in Figures 13 and 14, respectively. In the KAI feature, trends were investigated on a total of three lateral lineations contained within two depositional units; in the DAL feature, trends were investigated on a total of five lateral lineations contained within three depositional units. While some units loosely suggest a trend of decreasing particle size with increasing lateral distance from the vent (e.g., Figure 14c), other units showed no apparent trend (e.g., Figure 14e) or the opposite trend, with grain sizes loosely increasing with

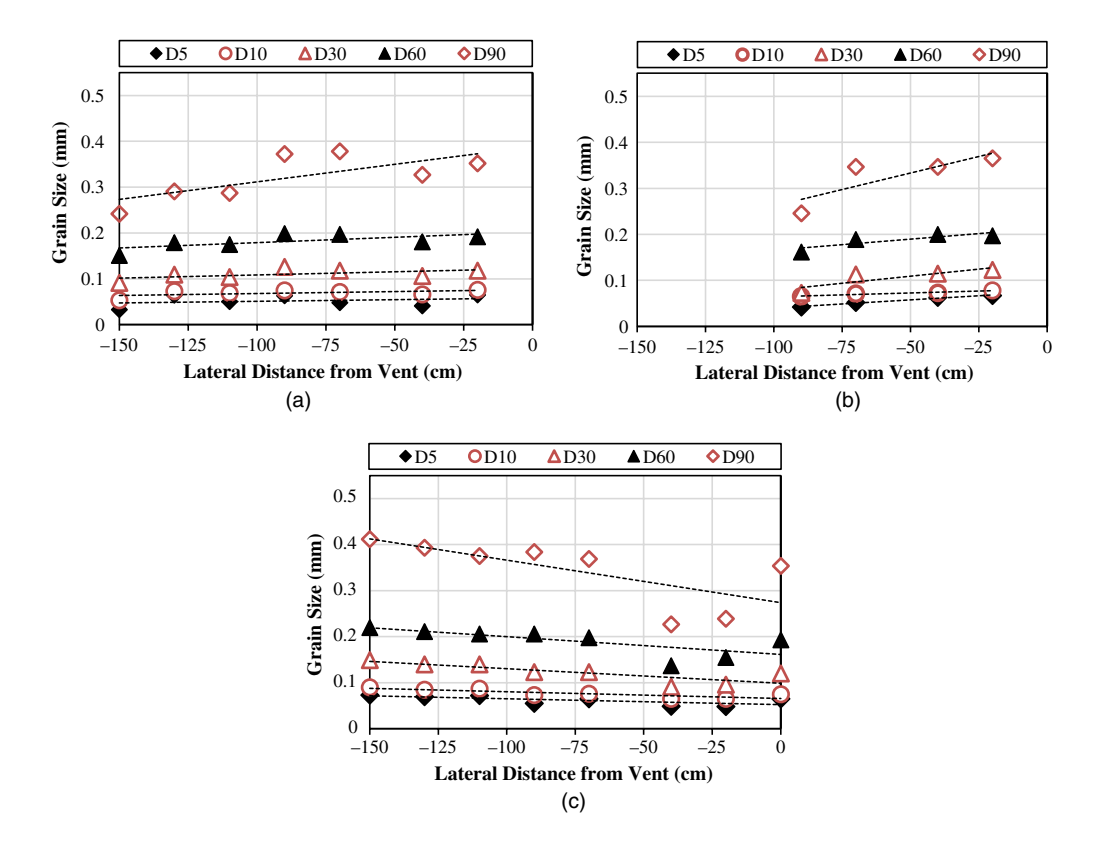


Figure 13. Analysis of particle-size trends in the lateral direction in the KAI trench along lineations of constant relative elevation: (a) base of first (oldest) unit, (b) top of first (oldest) unit, and (c) top of fifth (youngest) unit. Negative distances indicate that samples are left of the source vent (i.e., feeder dike), as viewed from the trench perspective mapped in Figure 5. The locations of samples plotted above, and their respective ejecta units, are also shown in Figure 5.

distance from the vent (e.g., Figure 13c). Furthermore, there was no relationship between the presence of fining-outward trends and either the vertical location within a unit or the source stratum's gradation.

In summary, particle-size gradation trends in both the vertical and lateral directions were unreliable for identifying episodes of liquefaction in the features investigated. The lack of reliable trends may be due to heterogeneities in the source stratum or to variations in the ejection velocity and mixing energy imparted during fluidization, among other factors. Regardless, results from the study sites indicate that in the absence of silt drapes, it would be very difficult to discern recurrent liquefaction or to accurately define the number of liquefaction episodes. As previously discussed, this, in turn, could lead to misinterpretation of the characteristics of the causative earthquake(s). Given that the features studied herein were recently deposited and minimally disturbed by weathering, spatial trends in particle gradation may be unreliable indicators of episodic liquefaction in older, more disturbed paleoliquefaction features.

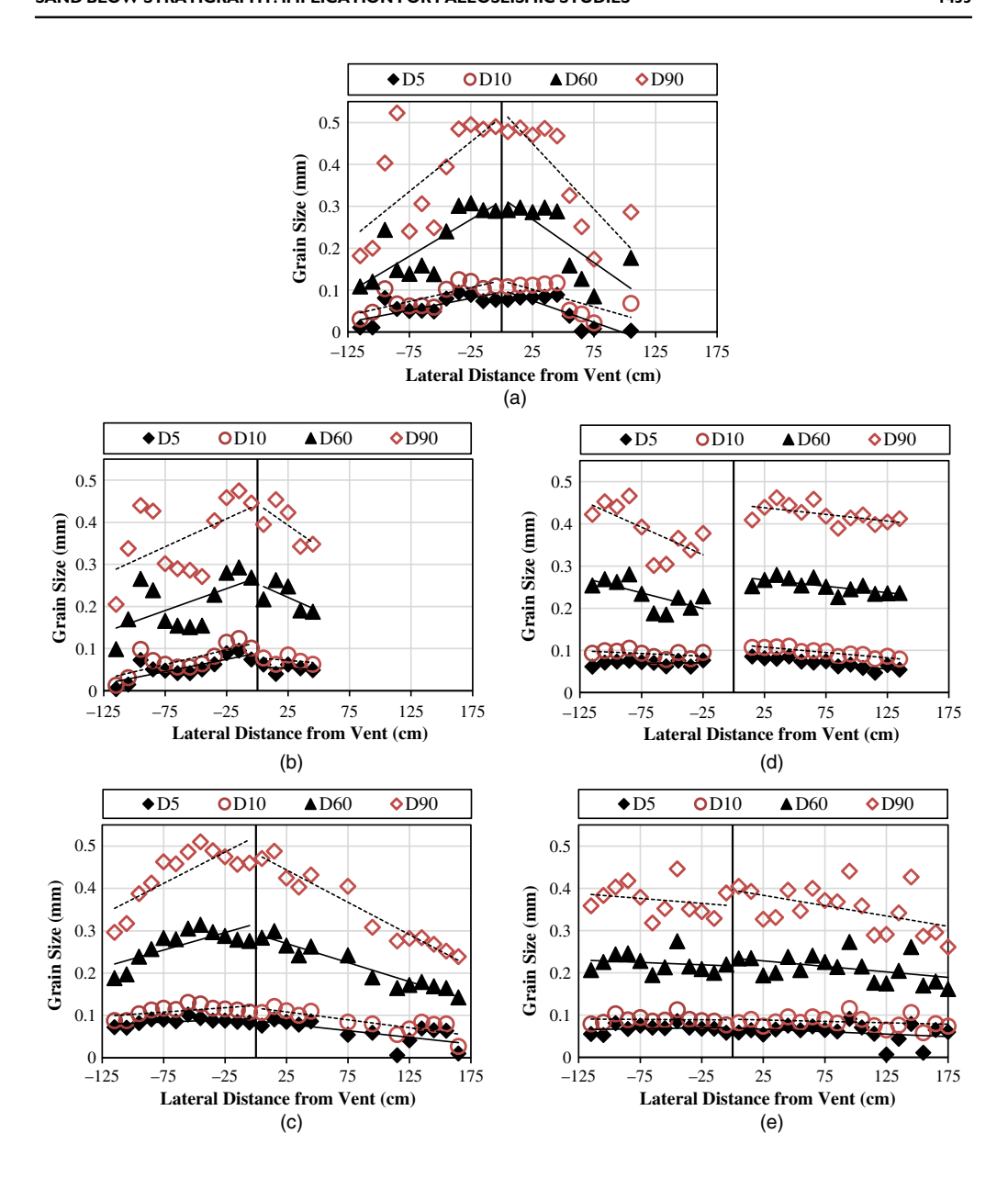


Figure 14. Analysis of particle-size trends in the lateral direction in the DAL trench along lineations of constant relative elevation: (a) top of third (youngest) unit, (b) top of second unit, (c) base of second unit, (d) top of first (oldest) unit, and (e) base of first (oldest) unit. Positive and negative distances indicate that samples are respectively right and left of the source vent (i.e., feeder dike), as viewed from the trench perspective mapped in Figure 6. The locations of samples plotted above, and their respective ejecta units, are also shown in Figure 6.

SUMMARY AND CONCLUSIONS

In regions where the return period of large events is longer than the duration of the historical seismicity catalog, results from paleoliquefaction studies often contribute significant inputs to seismic hazard analyses (e.g., NRC 2012, Petersen et al. 2014) to include the locations and magnitude-recurrence rates of moderate to large events. However, an accurate interpretation of the paleoliquefaction observations is more difficult where liquefaction was triggered by multiple earthquakes spaced closely in time. In this regard, deciphering whether a feature resulted from one earthquake or from multiple clustered earthquakes can significantly alter the results from paleoliquefaction studies. Accordingly, to better interpret paleoliquefaction evidence, a series of trenches were dug through recurrent liquefaction features formed during the 2010–2011 CES, with emphasis on discerning episodic liquefaction. The structure of blow material was mapped in detail, and extensive sampling was performed to analyze spatial trends in particle-size gradation. Multiple episodes of liquefaction were identified as layers of fine sand separated by silt drapes. The thickness of the silt drapes is shown to be directly correlated to the fines content of the liquefied source stratum. While these drapes provided a definitive demarcation of liquefaction episodes, their presence is dependent on the source stratum having sufficient fines to allow the drapes to form, and as such, the absence of silt drapes does not necessarily imply that a feature was produced by a single earthquake. In addition, there were no ubiquitous trends in the spatial sorting of grain sizes in the coarser fraction of the ejecta underlying silt drapes at the study sites, even though these strata were often 10 cm thick and flowed laterally up to several meters. While such trends have previously been used to identify episodic paleoliquefaction, the results of this study suggest that spatial trends may not manifest and, thus, may be unreliable for the interpretation of paleoliquefaction features. This study investigated unique modern analogs to recurrent paleoliquefaction evidence, and the resulting findings could have important implications for interpretation of seismic hazards in the CEUS and elsewhere. However, we note that the source strata for all the sites studied had similar modes of deposition and geologic origin. As a result, it cannot be stated with certainty that compound sand boils formed from deposits having differing compositions and geomorphologic origins will have the same stratigraphies as the features studied herein. However, many deposits hosting paleoliquefaction features worldwide have similar compositions and geomorphologies as those presented in this study (i.e., non-to-low plastic fluvial deposits), and thus the features could be expected to have similar stratigraphies.

ACKNOWLEDGMENTS

The authors wish to thank Brad Wham for assistance in trenching and Annie Liu for carrying out laser diffraction testing. Additionally, the fieldwork performed as part of this study was part of a broader study of the CES that involved numerous researchers, including Misko Cubrinovski, Brendon Bradley, Merrick Taylor, Thomas O'Rourke, Jonathan Bray, Mark Quigley, Brady Cox, Clint Wood, Sjoerd van Ballegooy, Mike Jacka, and others; their contributions and collaboration are gratefully acknowledged. The study presented herein is based on work supported by the National Science Foundation under Grant Numbers CMMI-1435494, CMMI-1724575, CMMI-1751216, and CMMI-1825189, as well as Pacific Earthquake Engineering Research Center Grant Number 1132-NCTRBM, U.S. Geological Survey Award Numbers G12AP- 20002 and G18AP-00006, and the

Earthquake Commission (EQC) Capability Building Fund. Also, we acknowledge the New Zealand GeoNet project and its sponsors EQC, GNS Science, and Land Information New Zealand (LINZ) for providing the earthquake occurrence data used in this study. However, any opinions, findings, and conclusions or recommendations expressed in this paper are those of the authors and do not necessarily reflect the views of the National Science Foundation, the U.S. Geological Survey, EQC, GNS Science, or LINZ.

REFERENCES

- Bastin, S., Quigley, M., and Bassett, K., 2015. Paleo-liquefaction in Christchurch, New Zealand, GSA Bulletin 127, 1348–1365.
- Bastin, S., Bassett, K., Quigley, M. C., Maurer, B. W., Green, R. A., Bradley, B. A., and Jacobson, D., 2016. Late Holocene liquefaction at sites of contemporary liquefaction during the 2010–2011 Canterbury Earthquake Sequence, *Bulletin of the Seismological Society of America* 106, 881–903.
- Beavan, J., Fielding, E., Motagh, M., Samsonov, S., and Donnelly, N., 2011. Fault location and slip distribution of the 22 February 2011 M_w6.2 Christchurch, New Zealand, earthquake from geodetic data, *Seismological Research Letters* 82, 789–99.
- Berrill, J. B., Mulqueen, P. C., and Ooi, E. T. C., 1994. Liquefaction at Kaiapoi in the 1901 Cheviot, New Zealand, earthquake, *Bulletin of the New Zealand National Society for Earthquake Engineering* 27, 178–189.
- Brown, L. J., Beetham, R. D., Paterson, B. R., and Weeber, J. H., 1995. Geology of Christchurch, New Zealand, *Environmental and Engineering Geoscience* 1, 427–488.
- Bucci, M. G., Almond, P., Villamor, P., Ries, W., Smith, C., and Tuttle, M., 2017. When the earth blisters: Exploring recurrent liquefaction features in the coastal system of Christchurch, New Zealand, *Terra Nova* **29**, 162–172.
- Canterbury Geotechnical Database, 2012. Aerial Photography, Map Layer CGD0100, 1 June 2012, available at https://canterburygeotechnicaldatabase.projectorbit.com. (last accessed 1 December 2012).
- Counts, R., and Obermeier, S., 2012. Subtle seismic signatures: using small-scale features and ground fractures as indicators of paleoseismicity, in *Recent Advances in North American Paleoseismology and Neotectonics East of the Rockies* (R. T. Cox, M. P. Tuttle, O. S. Boyd, and J. Locat, eds.), Geological Society of America, Boulder, CO, 203–219.
- Cox, R. T., Hill, A. A., Larsen, D., Holzer, T., Forman, S. L., Noce, T., Gardner, C., and Morat, J., 2007. Seismotectonic implications of sand blows in the southern Mississippi embayment, *Engineering Geology* **89**, 278–299.
- Cubrinovski, M., and Green, R. A., 2010. Geotechnical reconnaissance of the 2010 Darfield (Canterbury) earthquake, *Bulletin of the New Zealand Society for Earthquake Engineering* **43**, 243–320.
- Cubrinovski, M, Bray, J. D., Taylor, M., Giorgini, S., Bradley, B., Wotherspoon, L., and Zupan, J., 2011a. Soil liquefaction effects in the central business district during the February 2011 Christchurch earthquake, *Seismological Research Letters* 82, 893–904.
- Cubrinovski, M., Bradley, B., Wotherspoon, L., Green, R., Bray, J., Woods, C., Pender, M.,
 Allen, J., Bradshaw, A., Rix, G., Taylor, M., Robinson, K., Henderson, D., Giorgini, S.,
 Ma, K., Winkley, A., Zupan, J., O'Rourke, T., DePascale, G., and Wells, D., 2011b.
 Geotechnical aspects of the 22 February 2011 Christchurch earthquake, Bulletin of the
 New Zealand Society for Earthquake Engineering 43, 205–226.

Cubrinovski, M., Robinson, K., Taylor, M., Hughes, M. M., and Orense, R., 2012. Lateral spreading and its impacts in urban areas in the 2010-2011 Christchurch earthquakes, *New Zealand Journal of Geology and Geophysics* **55**, 255–269.

- DeGroot, M. H., and Schervish, M. J., 2012. *Probability and Statistics*, 4th edition, Pearson Education, London, United Kingdom, 912 pp.
- Environment Canterbury (ECan), 2004. Solid facts on Christchurch liquefaction, Environment Canterbury, Christchurch, New Zealand, available at http://ecan.govt.nz/publications/General/soid-facts-christchurch-liquefaction.pdf (last accessed 10 June 2019).
- GeoNet, 2012. New Zealand earthquake occurrence data: Felt quakes, available at http://geonet.org.nz/ (last accessed 10 June 2019).
- Green, R. A., and Bommer, J. J., 2019. What is the smallest earthquake magnitude that needs to be considered in assessing liquefaction hazard? *Earthquake Spectra* (in press).
- Green, R. A., Obermeier, S. F., and Olson, S. M., 2005. Engineering geologic and geotechnical analysis of paleoseismic shaking using liquefaction effects: Field examples, *Engineering Geology* **76**, 263–293.
- Green, R. A., Allen, A., Wotherspoon, L., Cubrinovski, M., Bradley, B., Bradshaw, A., Cox, B., and Algie, T., 2011a. Performance of levees (stopbanks) during the 4 September M_w7.1 Darfield and 22 February 2011 M_w6.2 Christchurch, New Zealand, earthquakes, *Seismological Research Letters* 82, 939–949.
- Green, R. A., Wood, C., Cox, B., Cubrinovski, M., Wotherspoon, L., Bradley, B., Algie, T., Allen, J., Bradshaw, A., and Rix, G., 2011b. Use of DCP and SASW tests to evaluate lique-faction potential: predictions vs. observations during the recent New Zealand earthquakes, *Seismological Research Letters* 82, 927–938.
- Green, R. A., Bommer, J. J., Rodriguez-Marek, A., Maurer, B., Stafford, P., Edwards, B., Kruiver, P. P., de Lange, G., and van Elk, J., 2018. Addressing limitations in existing 'simplified' liquefaction triggering evaluation procedures: application to induced seismicity in the Groningen gas field, *Bulletin of Earthquake Engineering*.
- Hough, S. E., 2011. Presentation made to the Independent Expert Panel on NMSZ Earthquake Hazard, 14 March 2011, FedEx Institute of Technology, Memphis, TN.
- Idriss, I. M., and Boulanger, R. W., 2008. *Soil Liquefaction during Earthquakes*, Earthquake Engineering Research Institute, Oakland, CA, 261 pp.
- Ishihara, K., 1985. Stability of natural deposits during earthquakes, in *Proceedings of the 11th International Conference on Soil Mechanics and Foundation Engineering*, CRC Press, Boca Raton, FL, 321–376.
- Kam, W. Y., Akguzel, U., and Pampanin, S., 2011. 4 Weeks on: Preliminary Reconnaissance Report from the Christchurch 22 Feb 2011 6.3M_w Earthquake, Tech. Rep., New Zealand Society of Earthquake Engineering, Wellington, New Zealand.
- Maurer, B. W., Green, R. A., Cubrinovski, M., and Bradley, B. A., 2014. Evaluation of the liquefaction potential index for assessing liquefaction hazard in Christchurch, New Zealand, *Journal of Geotechnical and Geoenvironmental Engineering* **140**.
- Maurer, B. W., Green, R. A., Cubrinovski, M., and Bradley, B., 2015a. Assessment of CPT-based methods for liquefaction evaluation in a liquefaction potential index framework, *Géotechnique* **65**, 328–336.
- Maurer, B. W., Green, R. A., Cubrinovski, M., and Bradley, B. A., 2015b. Fines-content effects on liquefaction hazard evaluation for infrastructure during the 2010-2011 Canterbury, New Zealand earthquake sequence, *Soil Dynamics and Earthquake Engineering* **76**, 58–68.

- Maurer, B. W., Green, R. A., Quigley, M. C., and Bastin, S., 2015c. Development of magnitude-bound relations for paleoliquefaction analyses: New Zealand case study, *Engineering Geology* **197**, 253–266.
- New Zealand Geotechnical Database, 2012. Aerial Photography, Map Layer CGD0100 1 June 2012, available at https://www.nzgd.org.nz/ (last accessed 12 April 2018).
- Nuclear Regulatory Commission (NRC), 2012. Central and Eastern United States Seismic Source Characterization for Nuclear Facilities, Tech. Rep. NUREG-2115, Nuclear Regulatory Commission, Rockville, MD.
- Obermeier, S., 1989. The New Madrid Earthquakes: An Engineering-Geologic Interpretation of Relict Liquefaction Features, Tech. Rep. 1336-B, U.S. Geological Survey, Denver, CO.
- Obermeier, S., 1996. Use of liquefaction-induced features for paleoseismic analysis an overview of how seismic liquefaction features can be distinguished from other features and how their regional distribution and properties of source sediment can be used to infer the location and strength of Holocene paleo-earthquakes, *Engineering Geology* 44, 1–76.
- Obermeier, S. F., and Dickenson, S. E., 2000. Liquefaction evidence for the strength of ground motiosn resulting from the late Holocene Cascadia subduction earthquakes, with emphasis on the event of 1700 A.D., *Bulletin of the Seismological Society of America* **90**, 876–896.
- Obermeier, S., Bleuer, N., Munson, C., Munson, P., Martin, W., McWilliams, K., Tabaczynski, D., Odum, J., Rubin, M., and Eggart, D., 1991. Evidence of strong earthquake shaking in the lower Wabash Valley from prehistoric liquefaction features, *Science* **251**, 1061–1063.
- Obermeier, S. F., Olson, S. M., and Green, R. A., 2005. Field occurrences of liquefaction-induced features: a primer for engineering and geologic analysis of paleoseismic shaking, *Engineering Geology* **76**, 209–234.
- Obermeier, S. F., Pond, E. C., Olson, S. M., Green, R. A., Mitchell, J. K., and Stark, T. D., 2001. Paleoliquefaction Studies in Continental Settings: Geologic and Geotechnical Factors in Interpretations and Back-Analysis, Tech. Rep. 01-029, U.S. Geological Survey, Denver, CO.
- Olson, S. M., Green, R. A., and Obermeier, S. F., 2005a. Revised magnitude bound relation for the Wabash Valley Seismic Zone of the central United States, *Seismological Research Letters* **76**, 756–771.
- Olson, S. M., Green, R. A., and Obermeier, S. F., 2005b. Geotechnical analysis of paleoseismic shaking using liquefaction features: A major updating, *Engineering Geology* 76, 235–261.
- Petersen, M. D., Moschetti, M. P., Powers, P. M., Mueller, C. S., Haller, K. M., Frankel, A. D., Zeng, Y., Rezaeian, S., Harmsen, S. C., Boyd, O. S., Field, N., Chen, R., Rukstales, K. S., Luco, N., Wheeler, R. L., Williams, R. A., and Olsen, A. H., 2014. *Documentation for the 2014 Update of the United States National Seismic Hazard Maps, Tech. Rep. 2014-1091*, U.S. Geological Survey, Denver, CO.
- Quigley, M. C., Bastin, S., and Bradley, B. A., 2013. Recurrent liquefaction in Christchurch, New Zealand, during the Canterbury earthquake sequence, *Geology* **41**, 419–422.
- Robinson, K., Cubrinovski, M., and Bradley, B. A., 2014. Lateral spreading displacements from the 2010 Darfield and 2011 Christchurch earthquakes, *International Journal of Geotechnical Engineering* **8**, 441–448.
- Saucier, R. T., 1989. Evidence for episodic sand-blow activity during the 1811-1812 New Madrid (Missouri) earthquake series, *Geology* **17**, 103–106.
- Sims, J. D., and Garvin, C. D., 1995. Recurrent liquefaction induced by the 1989 Loma Prieta earthquake and 1990 and 1991 aftershocks: Implications for paleoseismicity studies, *Bulletin of the Seismological Society of America* **85**, 51–65.

Talwani, P., and Schaeffer, W. T., 2001. Recurrence rates of large earthquakes in the South Carolina Coastal Plain based on paleoliquefaction data, *Journal of Geophysical Research* **106**, 6621–6642.

- Tuttle, M. P., 2001. The use of liquefaction features in paleoseismology: lessons learned in the New Madrid seismic zone, central United States, *Journal of Seismology* **5**, 361–380.
- Tuttle, M. P., 2012. Paleoliquefaction lessons learned from the 2010–2011 Canterbury, New Zealand, earthquakes, in *Proceedings of the Geological Society of America Annual Meeting*, 4–7 November, 2012, Charlotte, NC.
- Tuttle, M., and Hartleb, R., 2012. CEUS Paleo-liquefaction Database, Uncertainties Associated with Paleo-liquefaction Data, and Guidance for Seismic Source Characterization: Central and Eastern United States Seismic Source Characterization for Nuclear Facilities, Appendix E, NUREG-2115, U.S. Nuclear Regulatory Commission (NRC), Rockville, MD.
- Tuttle, M. P., Dyer-Williams, K., and Barstow, N. L., 2002a. Paleoliquefaction study of the Clarendon-Lindon fault system, western New York State, *Tectonophysics* **353**, 263–286.
- Tuttle, M. P., Schweig, E. S., Sims, J. D., Lafferty, R. H., Wolf, L. W., and Haynes, M. L., 2002b. The earthquake potential of the New Madrid Seismic Zone, *Bulletin of the Seismological Society of America* 92, 2080–2089.
- Tuttle, M. P., Schweig, E. S., Campbell, J., Thomas, P. M., Sims, J. D., and Lafferty, R. H., 2005. Evidence for New Madrid earthquakes in A.D. 300 and 2350 B.C., *Seismological Research Letters* 76, 489–501.
- Tuttle, M. P., Villamore, P., Almond, P., Bastin, S., Bucci, M. G., Langridge, R., Clark, K., and Hardwick, C. M., 2017. Liquefaction induced during the 2010–2011 Canterbury, New Zealand, Earthquake Sequence and lessons learned for the study of paleoliquefaction features, Seismological Research Letters 88, 1403–1414.
- van Ballegooy, S., Malan, P., Lacrosse, V., Jacka, M. E., Cubrinovski, M., Bray, J. D., O'Rourke, T. D., Crawford, S. A., and Cowan, H., 2014. Assessment of liquefaction-induced land damage for residential Christchurch, *Earthquake Spectra* **30**, 31–55.
- Wotherspoon, L. M., Pender, M. J., and Orense, R. P., 2012. Relationship between observed liquefaction at Kaiapoi following the 2010 Darfield earthquake and former channels of the Waimakariri River, *Engineering Geology* **125**, 45–55.

(Received 18 April 2018; Accepted 18 December 2018)